Preprints of the 21st IFAC World Congress (Virtual)
Berlin, Germany, July 12-17, 2020

Integrated Active Control of Electric Vehicles

Cuauhtémoc Acosta Lúa, * **Bernardino Castillo–Toledo,** ** **and Stefano Di Gennaro** ***,****

* *Departamento de Ciencias Tecnológicas, Centro Universitario de la Ciénega, Universidad de Guadalajara, Av. Universidad No. 1115, Col. Lindavista, Ocotlán, 47820, Jalisco, México (e.mail:* `cuauhtemoc.acosta@cuci.udg.mx`*).*

** *Department of Electrical Engineering, CINVESTAV–IPN Guadalajara, Av. del Bosque 1145 Col. El Bajío, CP 45019, México (e.mail:* `toledo@gdl.cinvestav.mx`*).*

*** *Department of Information Engineering, Computer Science and Mathematics, Via Vetoio, Loc. Coppito, 67100 L'Aquila, Italy. (e.mail:* `stefano.digennaro@univaq.it`*).*

**** *Center of Excellence DEWS, University of L'Aquila, Via Vetoio, Loc. Coppito, 67100 L'Aquila, Italy*

Abstract: This work describes how it is possible to integrate active chassis control actions in an electric vehicle. A vehicle with Active Front Steering (AFS) is considered, which imposes an incremental steer angle to the front wheels. Using Permanent Magnet Synchronous Motors (PMSMs) as powertrain, fitting on the left/right wheel axle shafts, it is possible to impose not only a desired longitudinal traction, but also an appropriate active yaw torque, so mimicking a classic Rear Torque Vectoring (RTV). The AFS, along with the RTV, allow imposing a desired behavior for the active chassis control of the vehicle, so improving its safety.

Keywords: Nonlinear control, Permanent magnet synchronous motors, Ground vehicles, Active control, Active Front Steering, Rear Torque Vectoring.

1. INTRODUCTION

Electric vehicles (EVs) can help in solving the problems of modern cities, facing the problem of pollution. At the same time, they represent an appealing potentiality for improving driving comfort, safety and performance of the vehicle. The emerging architecture with independent electric motors for each wheel attracts the interest the industrial developers. In fact, the torque characteristics, the energy optimization aspects, the simplification of the chassis control architecture and the vehicle structural flexibility are positive aspects in favour of this solution Hori (2004), Wang et al. (2011).

Among the other benefits, this technical solution allows improving the chassis control of the vehicle. The global chassis control supervises the longitudinal, lateral, vertical and yaw dynamics of the vehicle to avoid dangerous situations, so improving safety, as well as maneuverability and comfort Shuai et al. (2014), Ni et al. (2017), Ji et al. (2018). Usually, lateral and yaw control are decoupled from the control of the other dynamics, and can be achieved via devices like Active Front Steering (AFS) and Rear Torque Vectoring (RTV) Acosta–Lúa et al. (2007) – Etienne et al. (2019). AFS imposes an incremental steer angle to the front wheels, whereas RTV imposes a yaw torque to the vehicle. In order to implement this latter actuator, different solutions are possible, such as the economic differential braking or the more expensive active differentials. The use of electric drives allows implementing a simpler architecture for the RTV. In fact, using Permanent Magnet Synchronous Motors (PMSMs) as powertrain, fitting on the left/right wheel axle shafts, it is possible to impose at the same time a desired longitudinal traction and also the appropriate active yaw torque, so mimicking a classic RTV.

The main objective of the paper is to show how this can be achieved. For, it is shown how the PMSMs used as powertrain can be controlled to provide at the same time the required longitudinal traction and, using the different slips of the rear left and right wheels imposed by the motors, the required yaw torque necessary to control the yaw dynamics of the vehicle. The active control is then completed with the design of the AFS necessary to impose the desired lateral velocity. Finally, its is shown how the

[1] This paper has been also partially supported by the European Project ECSEL–JU RIA–2018 "Comp4Drones", and by the Project "Coordination of autonomous unmanned vehicles for highly complex performances", Executive Program of Scientific and Technological Agreement between Italy (Ministry of Foreign Affairs and International Cooperation, Italy) and Mexico (Mexican International Cooperation Agency for the Development), SAAP3.

rear left and right wheel angular velocities can be imposed controlling the voltage of the PMSMs. The performance of the proposed controller is finally tested by simulations.

There are a number of papers dealing with active chassis control (see e.g. Acosta–Lúa et al. (2007) and references therein), and many papers on the control of electric vehicles (see e.g. Shuai et al. (2014), Ni et al. (2017) and references therein), but only few papers study the integration of active chassis control actions with the control of the longitudinal speed of an EV. In Kim et al. (2008), a four–wheel-drive hybrid electric vehicle is considered, with rear motors, and a fuzzy–rule–based control is proposed. In Kim et al. (2013), in–wheel motor EVs are considered, with a torque vectoring and electronic stability control to improve stability and maneuverability. An integrated chassis control systems is designed to coordinate the control actions of individual chassis control systems in Fu et al. (2018). Electric traction and intelligent chassis are combined in Liu et al. (2015). Ming et al. (2015) consider an integrated chassis control method with optimal tire force distribution. More recently, Zhang et al. (2019) propose a cooperative chassis control system controlling the longitudinal motion in accordance with the yaw movement for EVs. Furthermore, Lv et al. (2019) propose a CPS–based framework for co–design optimization of an automated electric vehicle with different driving styles. These papers do use combined AFS and RTV actuators in an EV. The present paper presents, as main contribution, an integrated active chassis controller combining AFS and RTV for an EV equipped by PMSMs, ensuring the tracking of suitable reference for the longitudinal, lateral and yaw dynamics.

The paper is organized as follows. In Section 2, the mathematical model of an EV is recalled, and the problem for active chassis control is formulated. In Section 3, a controller is designed to solve this problem, whereas in Section 4 some simulations results are given, showing the effectiveness of the proposed solution. Finally, some conclusions are given, along with some future activities.

2. MATHEMATICAL MODEL OF AN ELECTRIC VEHICLE

The mathematical model of a ground vehicle can be obtained considering a rigid body connected to the ground through tires. The vehicle dynamics are very complex but, for the aim of the attitude control design, it is possible to consider the simple model describing the yaw and lateral dynamics, the so–called single track or bicycle model (Wong et al. (1978)). It represents the essence of the dynamics to be controlled, whilst the remaining dynamics, coupled with them, are considered as external disturbances. On the basis of such a model one can design controllers whose effectiveness can be tested and validated on more complex models, unsuitable for control design, which are available for describing accurately the vehicle dynamics.

The active actuators considered in this work are the AFS, which imposes an incremental steer angle δ_c, and a differential yaw torque M_z implementing the RTV. This latter will be realized via PMSMs placed on the rear axel, as better discussed below. The vehicle dynamics are

$$\begin{aligned} m(\dot v_x - v_y\omega_z) &= ma_x = \mu_x(F_{x,f}+F_{x,r}) + F_{d,x} \\ m(\dot v_y + v_x\omega_z) &= ma_y = \mu_y(F_{y,f}+F_{y,r}) + F_{d,y} \\ J_z\dot\omega_z &= \mu_y(F_{y,f}l_f - F_{y,r}l_r) + M_z + M_{d,z} \end{aligned} \tag{1}$$

where m, J_z are the vehicle mass and inertia momentum, l_f, l_r are the front and rear vehicle length, v_x, v_y are the longitudinal, lateral velocities of the vehicle center of mass, and ω_z is the yaw rate. Moreover, μ_x, μ_y are the longitudinal/lateral tire–road friction coefficients. Furthermore, a_x, a_y are the longitudinal/lateral accelerations, $F_{x,f}$, $F_{x,r}$ and $F_{y,f}$, $F_{y,r}$ are the front/rear longitudinal/lateral forces, M_z is the yaw moment, resulting from controller's active braking, F_d, is an external perturbing force acting on the vehicle, with $F_{d,x}$, $F_{d,y}$ the x, y components, and $M_{d,z}$ is corresponding torque. The disturbance F_d is typically due to environmental actions, such as the wind.

The longitudinal and lateral forces $F_{x,f}$, $F_{x,r}$, $F_{y,f}$, $F_{y,r}$ are normalized with respect to the tire–road friction coefficients μ_x, μ_y. Moreover, the lateral forces $F_{y,f}$, $F_{y,r}$ depend on the front and rear tire slip angles

$$\alpha_f = \delta_d + \delta_c - \frac{v_y + l_f\omega_z}{v_x}, \quad \alpha_r = -\frac{v_y - l_r\omega_z}{v_x}$$

where δ_d, δ_c are the steering wheel angle due to the driver and to the angle imposed by the AFS. Note that if $\delta_d = 0$, the vehicle is autonomous.

There are many tire models, and the approach followed here does not depend on them. To fix the ideas, and without loss of generality, in this paper we consider the well–known Pacejka model Pacejka et al. (2005)

$$\begin{aligned} F_{y,j}(\alpha_j) &= \mathcal{F}_{y,j}(\alpha_j) \\ \mathcal{F}_{y,j} &= D_{y,j}\sin\Big[C_{y,j}\arctan\Big(B_{y,j}\alpha_j \\ &\qquad - E_{y,j}\big(B_{y,j}\alpha_j - \arctan(B_{y,j}\alpha_j)\big)\Big)\Big] \end{aligned}$$

$j = f, r$, with $B_{y,j}$, $C_{y,j}$, $D_{y,j}$, $E_{y,j}$ experimental parameters (Pacejka et al. (2005)). The nonlinearities of the simple model (1) arise from these characteristics of the tires, in addition to the gyroscopic terms $v_x\omega_z$, $v_y\omega_z$. For convenience, in the following it will be used the notation

$$F_{y,f}(\alpha_f) = F_{y,f}(\delta, v_y, \omega_z), \quad F_{y,r}(\alpha_r) = F_{y,r}(v_y, \omega_z)$$

where δ is the applied steering wheel angle ($\delta = \delta_d$ when no AFS is considered, whereas $\delta = \delta_d + \delta_c$ when the AFS is present).

The tire front/rear longitudinal forces $F_{x,f}$, $F_{x,r}$ have expressions formally similar to that of $F_{y,f}$, $F_{y,r}$, but they depend on the so–called longitudinal slips λ_f, λ_r. For the front wheel the mechanical equation and the longitudinal force are

$$\begin{aligned} \dot\omega_f &= \frac{1}{J_f}\Big(T_f - T_{b,f} - T^v_{s,r} - r_f(F_{x,f} + F^v_{x,f})\Big) \\ F_{x,f}(\lambda_f) &= F_{x,f}(v_x, \omega_f) = \mathcal{F}_{x,f}(\lambda_f) \\ \lambda_f &= \frac{v_x - r_f\omega_f}{v_x} = 1 - r_f\frac{\omega_f}{v_x} \\ \mathcal{F}_{x,f} &= D_{x,f}\sin\Big[C_{x,f}\arctan\Big(B_{x,f}\lambda_f \\ &\qquad - E_{x,f}\big(B_{x,f}\lambda_f - \arctan(B_{x,f}\lambda_f)\big)\Big)\Big] \end{aligned} \tag{2}$$

with ω_f the front wheel angular velocity, T_f the torque generated by the front powertrain, $T_{b,f}$ the torque applied by the brake to the wheel, $F_{x,f}$ the front tractive force,

$F^v_{x,f}$ the viscous force at the contact patch, $T^v_{s,r}$ the viscous torque on the axle, and r_f the so–called equivalent radius of the front tire. Finally, $B_{x,f}$, $C_{x,f}$, $D_{x,f}$, $E_{x,f}$ are experimental parameters. Clearly, also in this case the tire model could be different.

In this work we consider, without loss of generality, a rear wheel drive, i.e. $T_f = 0$, and a negligible viscous force/torque $T^v_{s,r}$, $F^v_{x,f}$. As far as the rear axle is concerned, in this work the rear powertrain is constituted by two PMSMs, fit on the left/right wheel axle shafts. It is assumed that these motors satisfy the usual hypotheses (linear magnetic materials, symmetry of the rotor and between the two phases, nonlinear flux density distribution due to air gap geometry only, negligible magnetic hysteresis and Foucault currents) under which it can be satisfactorily modeled by means of the usual simplified equations (Krause et al. (2017), Leonard et al. (1985)). Moreover, the motors are assumed with no saliencies and with sinusoidal flux density distributions. In the equations below, ℓ, $\imath$ stand for the left and right PMSM, respectively, whose dynamics in the (d,q) rotor frame are (Krause et al. (2017), Leonard et al. (1985))

$$\begin{aligned}
\frac{di_{d,\ell}}{dt} &= -\frac{R_\ell}{L_\ell} i_{d,\ell} + p\omega_{r,\ell} i_{q,\ell} + \frac{1}{L_\ell} v_{d,\ell} \\
\frac{di_{q,\ell}}{dt} &= -\frac{R_\ell}{L_\ell} i_{q,\ell} - p\omega_{r,\ell} i_{d,\ell} - p\frac{\Phi_\ell}{L_\ell}\omega_{r,\ell} + \frac{1}{L} v_{q,\ell} \\
\frac{di_{d,\imath}}{dt} &= -\frac{R_\imath}{L_\imath} i_{d,\imath} + p\omega_{r,\imath} i_{q,\imath} + \frac{1}{L_\imath} v_{d,\imath} \\
\frac{di_{q,\imath}}{dt} &= -\frac{R_\imath}{L_\imath} i_{q,\imath} - p\omega_{r,\imath} i_{d,\imath} - p\frac{\Phi_\imath}{L_\imath}\omega_{r,\imath} + \frac{1}{L} v_{q,\imath}
\end{aligned} \tag{3}$$

where $v_\ell = \begin{pmatrix} v_{d,\ell} & v_{q,\ell} \end{pmatrix}^T$, $v_\imath = \begin{pmatrix} v_{d,\imath} & v_{q,\imath} \end{pmatrix}^T$, $i_\ell = \begin{pmatrix} i_{d,\ell} & i_{q,\ell} \end{pmatrix}^T$, $i_\imath = \begin{pmatrix} i_{d,\imath} & i_{q,\imath} \end{pmatrix}^T$ the stator voltage and current vectors, R_ℓ, $R_\imath$ are the stator resistances, L_ℓ, $L_\imath$ are the inductances, p the pole pair number, Φ_ℓ, $\Phi_\imath$ the fluxes produced by the permanent magnets. The mechanical equations are given by

$$\begin{aligned}
\dot\omega_{r,\ell} &= \frac{1}{J_\ell}\Big(T_{r,\ell} - T_{b,r,\ell} - T^v_{s,r,\ell} - r_{r,\ell}(F_{x,r,\ell} + F^v_{x,r,\ell})\Big) \\
\dot\omega_{r,\imath} &= \frac{1}{J_\imath}\Big(T_{r,\imath} - T_{b,r,\imath} - T^v_{s,r,\imath} - r_{r,\imath}(F_{x,r,\imath} + F^v_{x,r,\imath})\Big)
\end{aligned} \tag{4}$$

where J_ℓ, $J_\imath$ are the inertias, $r_{r,\ell}$, $r_{r,\imath}$ are the equivalent radii of the rear tires, $T_{r,\ell} = p\Phi_\ell i_{q,\ell}$, $T_{r,\imath} = p\Phi_\imath i_{q,\imath}$ are the torques generated by the left/right PMSMs, and $T_{b,r,\ell}$, $T_{b,r,\imath}$ are the torques applied by the brakes to the wheels. The viscous forces $F^v_{x,r,\ell}$, $F^v_{x,r,\imath}$ at the contact patches and the viscous torques $T^v_{s,r,\ell} = f_\ell\omega_{r,\ell}$, $T^v_{s,r,\imath} = f_\imath\omega_{r,\imath}$ on the motor shafts are considered negligible. Moreover,

$$\begin{aligned}
F_{x,r,\ell}(\lambda_{r,\ell}) &= F_{x,r,\ell}(v_x,\omega_{r,\ell}) = \mathcal{F}_{x,r,\ell}(\lambda_{r,\ell}) \\
F_{x,r,\imath}(\lambda_{r,\imath}) &= F_{x,r,\imath}(v_x,\omega_{r,\imath}) = \mathcal{F}_{x,r,\imath}(\lambda_{r,\imath}) \\
\lambda_{r,\ell} &= 1 - r_{r,\ell}\frac{\omega_{r,\ell}}{v_x}, \qquad \lambda_{r,\imath} = 1 - r_{r,\imath}\frac{\omega_{r,\imath}}{v_x} \\
\mathcal{F}_{x,r,h} &= D_{x,r,h}\sin\big[C_{x,r,h}\arctan\big(B_{x,r,h}\lambda_{r,h} \\
&\quad - E_{x,r,h}\big(B_{x,r,h}\lambda_{r,h} - \arctan(B_{x,r,h}\lambda_{r,h})\big)\big)\big]
\end{aligned}$$

$h = \ell, \imath$, are the left/right rear tractive forces, which determine the load torques $C_\ell = r_{r,\ell}F_{x,r,\ell}$, $C_\imath = r_{r,\imath}F_{x,r,\imath}$ for the PMSMs. Here, $B_{x,r,h}$, $C_{x,r,h}$, $D_{x,r,h}$, $E_{x,r,h}$, $h = \ell, \imath$, are experimental parameters. Therefore, the mechanical equations become

$$\begin{aligned}
\dot\omega_{r,\ell} &= \frac{1}{J_\ell}\Big(p\Phi_\ell i_{q,\ell} - T_{b,r,\ell} - r_{r,\ell}F_{x,r,\ell}\Big) \\
\dot\omega_{r,\imath} &= \frac{1}{J_\imath}\Big(p\Phi_\imath i_{q,\imath} - T_{b,r,\imath} - r_{r,\ell}F_{x,r,\imath}\Big).
\end{aligned} \tag{5}$$

Finally, let t_v be the vehicle track. Hence, the rear longitudinal force and the yaw moment determined by the rear tractive forces are

$$\begin{aligned}
F_{x,r} &= F_{x,r,\ell}(v_x,\omega_{r,\ell}) + F_{x,r,\imath}(v_x,\omega_{r,\imath}) \\
M_z &= \Big(F_{x,r,\ell}(v_x,\omega_{r,\ell}) - F_{x,r,\imath}(v_x,\omega_{r,\imath})\Big)\frac{t_v}{2}.
\end{aligned} \tag{6}$$

The smooth bounded function $F_{x,f}$, $F_{x,r}$, $F_{y,f}$, $F_{y,r}$ have some desired properties. In fact, they are odd functions

$$\phi F_{y,f}(\phi) > 0, \quad \phi F_{y,r}(\phi) > 0, \qquad \forall \phi \in \mathbb{R}\setminus\{0\}$$

and, in particular they have minimum/maximum value for certain values of ϕ. This is particularly interesting for $F_{y,f}$, which has a minimum/maximum value for certain values $\alpha_j = \pm\alpha_{j,\max}$, and is invertible with respect to α_j for $\alpha_j \in [-\alpha_{j,\max}, \alpha_{j,\max}]$. Hence, $F_{y,f}$ is invertible with respect to the control input δ_c, for $\alpha_f \in [-\alpha_{f,\max}, \alpha_{f,\max}]$, while for $\alpha_f < -\alpha_{f,\max}$, $\alpha_f > \alpha_{f,\max}$ it is common to consider the minimum/maximum value. Therefore, for a fixed value φ_0, the solution of

$$F_{y,f}(\alpha_f) = F_{y,f}(\delta_d + \delta_c, v_y, \omega_z) = \varphi_0$$

is unique and is given by

$$\delta_c = \begin{cases} -\delta_d + \dfrac{v_y + l_f\omega_z}{v_x} + F^{-1}_{y,f}(\varphi_0) & \text{if } \alpha_f \in [-\alpha_{f,\max}, \alpha_{f,\max}] \\ -\delta_d + \dfrac{v_y + l_f\omega_z}{v_x} \pm \alpha_{f,\max} & \text{otherwise.} \end{cases} \tag{7}$$

Under this hypothesis of invertibility, it is possible to consider as control input the difference

$$\Delta_c = F_{y,f}(\delta_d + \delta_c, v_y, \omega_z) - F_{y,f}(\delta_d, v_y, \omega_z) \tag{8}$$

instead of δ_c, so that equations (1) become

$$\begin{aligned}
\dot v_x &= v_y\omega_z + \frac{\mu_x}{m}\Big[F_{x,f}(v_x,\omega_f) + F_{x,r,\ell}(v_x,\omega_{r,\ell}) \\
&\qquad + F_{x,r,\imath}(v_x,\omega_{r,\imath})\Big] + \frac{1}{m}F_{d,x} \\
\dot v_y &= -v_x\omega_z + \frac{\mu_y}{m}\Big[F_{y,f}(\delta_d, v_y, \omega_z) + F_{y,r}(v_y,\omega_z)\Big] \\
&\quad + \frac{\mu_y}{m}\Delta_c + \frac{1}{m}F_{d,y} \\
\dot\omega_z &= \frac{\mu_y}{J_z}\Big[l_f F_{y,f}(\delta_d, v_y, \omega_z) - l_r F_{y,r}(v_y,\omega_z)\Big] \\
&\quad + \frac{\mu_y l_f}{J_z}\Delta_c + \Big(F_{x,r,\ell}(v_x,\omega_{r,\ell}) \\
&\qquad - F_{x,r,\imath}(v_x,\omega_{r,\imath})\Big)\frac{t_v}{2J_z} + \frac{1}{J_z}M_{d,z}
\end{aligned} \tag{9}$$

where (6) has been used. The mathematical model is given by (9) along with (2), (3), (4).

3. DESIGN OF AN ACTIVE CHASSIS CONTROL

The control aim is to design a controller such that v_x, ω_z globally track a reference longitudinal velocity $v_{x,\mathrm{ref}}$ and a yaw rate $\omega_{z,\mathrm{ref}}$, whereas the lateral velocity v_y is required to tend asymptotically a reference $v_{y,\mathrm{ref}}$. Considering the error variables $e_{v_x} = v_x - v_{x,\mathrm{ref}}$, $e_{v_y} = v_y - v_{y,\mathrm{ref}}$, $e_{\omega_z} = \omega_z - \omega_{z,\mathrm{ref}}$, the control problem consists of designing a controller such that $\lim_{t\to\infty} e_{v_x} = 0$, $\lim_{t\to\infty} e_{v_y} = 0$, $\lim_{t\to\infty} e_{\omega_z} = 0$. The components $i_{q,\ell}$, $i_{q,\imath}$ of the currents will be determined

imposing the desired RTV control M_z. A further control objective is to impose for the PMSMs some references $i_{d,\ell,\mathrm{ref}}$, $i_{d,\imath,\mathrm{ref}}$ for the "direct components" $i_{d,\ell}$, $i_{d,\imath}$ of the currents, which may depend on the wheel angular speeds $\omega_{r,\ell}$, $\omega_{r,\imath}$. This allows realizing the so–called "field weakening" at high speed. Therefore, when $\omega_{r,\ell}, \omega_{r,\imath} \leq \omega_n$ (ω_n is a nominal speed) then $i_{d,\ell,\mathrm{ref}} = 0$, $i_{d,\imath,\mathrm{ref}} = 0$, so maximizing the produced torque, whereas if $\omega_{r,\ell}, \omega_{r,\imath} > \omega_n$ then $i_{d,\ell,\mathrm{ref}} = i_{d,\ell,\mathrm{ref}}(\omega_{r,\ell})$, $i_{d,\imath,\mathrm{ref}} = i_{d,\imath,\mathrm{ref}}(\omega_{r,\imath})$.

The given control problem will be solved under the following assumptions.

Assumption 3.1. The signal δ_d is at least a C^2 function. ⋄

Assumption 3.2. The reference signals $v_{x,\mathrm{ref}}$, $v_{y,\mathrm{ref}}$, $\omega_{z,\mathrm{ref}}$, and their derivatives $\dot{v}_{x,\mathrm{ref}}$, $\dot{v}_{y,\mathrm{ref}}$, $\dot{\omega}_{z,\mathrm{ref}}$ are bounded. ⋄

Assumption 3.3. The tire–road friction coefficients μ_x, μ_y are different from zero. ⋄

Assumptions 3.1 and 3.2 require that the signal imposed to the steering wheel by the driver, and the references to be imposed to the vehicle are sufficiently regular. Assumption 3.3 means that, obviously, the tires have to be able to exert a nonzero force in the x or y direction in order to control the vehicle.

3.1 The Reference Generator

The references $v_{x,\mathrm{ref}}$, $v_{y,\mathrm{ref}}$, $\omega_{z,\mathrm{ref}}$ need to be feasible signals. To generate them, one can consider the dynamics of a 'reference vehicle' which mimics those of the real vehicle

$$\begin{aligned}
\dot{v}_{x,\mathrm{ref}} &= \omega_{z,\mathrm{ref}} v_{y,\mathrm{ref}} + \frac{\mu_{x,\mathrm{ref}}}{m_{\mathrm{ref}}}(F_{x,f,\mathrm{ref}} + F_{x,r,\mathrm{ref}}) \\
\dot{v}_{y,\mathrm{ref}} &= -\omega_{z,\mathrm{ref}} v_{x,\mathrm{ref}} + \frac{\mu_{y,\mathrm{ref}}}{m_{\mathrm{ref}}}(F_{y,f,\mathrm{ref}} + F_{y,r,\mathrm{ref}}) \\
\dot{\omega}_{z,\mathrm{ref}} &= \frac{\mu_{y,\mathrm{ref}}}{J_{z,\mathrm{ref}}}(F_{y,f,\mathrm{ref}} l_f - F_{y,r,\mathrm{ref}} l_r)
\end{aligned} \tag{10}$$

where the forces $F_{x,f,\mathrm{ref}}$, $F_{x,r,\mathrm{ref}}$, $F_{y,f,\mathrm{ref}}$, $F_{y,r,\mathrm{ref}}$, exerted by the tires of the reference vehicle, are similar to those of the real vehicle, but correspond to a "nominal" tire. In particular, $F_{y,r,\mathrm{ref}}$ is modified so that no tail–spins are possible in the reference vehicle. Usually, this is obtained ensuring that the rear tire characteristic is not decreasing after a certain value (corresponding to the maximal lateral force), as usually happens in a real tire. Moreover, m_{ref}, $J_{z,\mathrm{ref}}$ are the mass and inertia with respect to the z axis (z is oriented so that (x, y, z) is a right orthogonal frame), usually equal to the nominal values. Finally, $\mu_{x,\mathrm{ref}}$, $\mu_{y,\mathrm{ref}}$ are the reference tire–road friction coefficients in the x and y directions, and l_f, l_r are the distances from the vehicle center of gravity G_{ref} to the front and rear axels.

3.2 The Active Chassis Control Design

The controller which solves the control problem is derived below. The dynamics of the tracking errors e_{v_x}, e_{v_y}, e_{ω_z} are

$$\begin{aligned}
\dot{e}_{v_x} &= v_y\omega_z + \frac{\mu_x}{m}\Big[F_{x,f}(v_x,\omega_f) + F_{x,r,\ell}(v_x,\omega_{r,\ell}) \\
&\quad + F_{x,r,\imath}(v_x,\omega_{r,\imath})\Big] + \frac{1}{m}F_{d,x} - \dot{v}_{x,\mathrm{ref}} \\
\dot{e}_{v_y} &= -v_x\omega_z + \frac{\mu_y}{m}\Big[F_{y,f}(\delta_d, v_y, \omega_z) + F_{y,r}(v_y,\omega_z)\Big] \\
&\quad + \frac{\mu_y}{m}\Delta_c + \frac{1}{m}F_{d,y} - \dot{v}_{y,\mathrm{ref}} \\
\dot{e}_{\omega_z} &= \frac{\mu_y}{J_z}\Big[l_f F_{y,f}(\delta_d, v_y, \omega_z) - l_r F_{y,r}(v_y,\omega_z)\Big] + \frac{\mu_y l_f}{J_z}\Delta_c \\
&\quad + \Big(F_{x,r,\ell}(v_x,\omega_{r,\ell}) - F_{x,r,\imath}(v_x,\omega_{r,\imath})\Big)\frac{t_v}{2J_z} \\
&\quad + \frac{1}{J_z}M_{d,z} - \dot{\omega}_{z,\mathrm{ref}}.
\end{aligned}$$

The control can be calculated in order to impose a PI plus a super–twisting action (see Edwards et al. (1998) – Van et al. (2019)), i.e. such that one imposes the dynamics

$$\begin{aligned}
\dot{I}_{e_{v_x}} &= -\alpha_{2,x}\,\mathrm{sign}(e_{v_x}) - k_{i,x}e_{v_x} \\
\dot{e}_{v_x} &= -\alpha_{1,x}\,\lfloor e_{v_x}\rceil^{1/2} - k_{p,x}e_{v_x} + I_{e_{v_x}} \\
\dot{I}_{e_{v_y}} &= -\alpha_{2,y}\,\mathrm{sign}(e_{v_y}) - k_{i,y}e_{v_y} \\
\dot{e}_{v_y} &= -\alpha_{1,y}\,\lfloor e_{v_y}\rceil^{1/2} - k_{p,y}e_{v_y} + I_{e_{v_y}} \\
\dot{I}_{e_{\omega_z}} &= -\alpha_{2,z}\,\mathrm{sign}(e_{\omega_z}) - k_{i,z}e_{\omega_z} \\
\dot{e}_{\omega_z} &= -\alpha_{1,z}\,\lfloor e_{\omega_z}\rceil^{1/2} - k_{p,z}e_{\omega_z} + I_{e_{\omega_z}}
\end{aligned} \tag{11}$$

where $\lfloor e\rceil^{1/2} := |e|^{1/2}\,\mathrm{sign}(e)$, and $\alpha_{1,j}, \alpha_{2,j}, k_{p,j}, k_{i,j} > 0$, $4\alpha_{2,j}k_{i,j} > (9\alpha_{1,j}^2 + 8\alpha_{2,j})k_{p,j}^2$, $j = x, y, z$. In fact, imposing the dynamics

$$\begin{aligned}
\dot{I}_e &= -\alpha_2\,\mathrm{sign}(e) - k_i e \\
\dot{e} &= -\alpha_1|e|^{1/2}\,\mathrm{sign}(e) - k_p e + I_e
\end{aligned}$$

with $\alpha_1, \alpha_2, k_p, k_i > 0$, $4\alpha_2 k_i > (9\alpha_1^2 + 8\alpha_2)k_p^2$, implies that the (continuous but not differentiable in $e = 0$) Lyapunov candidate $V = E^T P E/2$, with

$$P = \begin{pmatrix} 4\alpha_2 + \alpha_1^2 & \alpha_1 k_p & -\alpha_1 \\ \alpha_1 k_p & 2k_i + k_p^2 & -k_p \\ -\alpha_1 & -k_p & 2 \end{pmatrix},\ E = \begin{pmatrix} |e|^{1/2}\,\mathrm{sign}(e) \\ e \\ I_e \end{pmatrix}$$

is such that (Moreno et al. (2008))

$$\dot{V} = -\frac{\alpha_1}{2}\frac{1}{|e|^{1/2}}E^T Q_1 E - k_p E^T Q_2 E$$

where

$$Q_1 = \begin{pmatrix} \alpha_1^2 + 2\alpha_2 & 0 & -\alpha_1 \\ 0 & 5k_p^2 + 2k_i & -3k_p \\ -\alpha_1 & -3k_p & 1 \end{pmatrix} > 0$$

$$Q_2 = \begin{pmatrix} 2\alpha_1^2 + \alpha_2 & 0 & 0 \\ 0 & k_p^2 + k_i & -k_p \\ 0 & -k_p & 1 \end{pmatrix} > 0.$$

As a consequence,

$$\dot{V} \leq \frac{(\lambda_{\min}^P)^{1/2}\lambda_{\min}^{Q_1}}{\lambda_{\max}^P}V^{1/2} - \frac{\lambda_{\min}^{Q_2}}{\lambda_{\max}^P}V$$

so that V and, hence, E converge to the origin in finite–time. This property is typical of super–twisting controllers. The dynamics (11) to be imposed by the control combine the classic PI action, which ensures the exponential convergence of the error trajectories, and the super–twisting action, which ensures the finite–time convergence: close to the origin, the super–twisting action is stronger, due to the fact that the super–twisting action is not Lipschitz in

the origin. On the other hand, the PI action is stronger far form the origin than the super–twisting action.

Under Assumption 3.3, one obtains the control that imposes the dynamics (11)

$$\begin{aligned} \Delta_c &= F_y^\circ \\ F_{x,r,\ell}(v_x,\omega_{r,\ell}) &= F_{x,r,\ell,\mathrm{ref}}(v_x,\omega_{r,\ell}) = \frac{1}{2}(F_x^\circ + \Delta_{F_x}) \\ F_{x,r,\imath}(v_x,\omega_{r,\imath}) &= F_{x,r,\imath,\mathrm{ref}}(v_x,\omega_{r,\imath}) = \frac{1}{2}(F_x^\circ - \Delta_{F_x}) \end{aligned} \tag{12}$$

where

$$\begin{aligned} \dot I_{e_{v_x}} &= -\alpha_{2,x}\,\mathrm{sign}(e_{v_x}) - k_{i,x}e_{v_x} \\ \dot I_{e_{v_y}} &= -\alpha_{2,y}\,\mathrm{sign}(e_{v_y}) - k_{i,y}e_{v_y} \\ \dot I_{e_{\omega_z}} &= -\alpha_{2,z}\,\mathrm{sign}(e_{\omega_z}) - k_{i,z}e_{\omega_z} \\ F_x^\circ &= -F_{x,f}(v_x,\omega_f) + \frac{1}{\mu_x}\Big(- mv_y\omega_z - m\alpha_{1,x}\left\lfloor e_{v_x}\right\rceil^{1/2} \\ &\quad - mk_{p,x}e_{v_x} + mI_{e_{v_x}} + m\dot v_{x,\mathrm{ref}} - F_{d,x}\Big) \\ F_y^\circ &= -F_{y,f}(\delta_d,v_y,\omega_z) - F_{y,r}(v_y,\omega_z) \\ &\quad + \frac{1}{\mu_y}\Big(mv_x\omega_z - m\alpha_{1,y}\left\lfloor e_{v_y}\right\rceil^{1/2} \\ &\quad - mk_{p,y}e_{v_y} + mI_{e_{v_y}} + m\dot v_{y,\mathrm{ref}} - F_{d,y}\Big) \\ \Delta_{F_x} &= \frac{2}{t_v}\Big(- \mu_y\Big(l_fF_{y,f}(\delta_d,v_y,\omega_z) - l_rF_{y,r}(v_y,\omega_z)\Big) \\ &\quad - \mu_y l_f\Delta_c - \alpha_{1,z}\left\lfloor e_{\omega_z}\right\rceil^{1/2} - k_{p,z}e_{\omega_z} \\ &\quad + I_{e_{\omega_z}} + J_z\dot\omega_{z,\mathrm{ref}} - M_{d,z}\Big). \end{aligned}$$

From (12), one gets the references to be imposed to the rear wheel angular velocities

$$\omega_{r,\ell,\mathrm{ref}} = \begin{cases} \dfrac{v_x}{r_{r,\ell}}\Big(1 - \mathcal{F}^{-1}_{x,r,\ell}(F_{x,r,\ell,\mathrm{ref}}(v_x,\omega_{r,\ell}))\Big) \\ \qquad\qquad \text{if } \lambda_{r,\ell} \in [-\lambda_{r,\max},\lambda_{r,\max}] \\ \dfrac{v_x}{r_{r,\ell}}\Big(1 \mp \lambda_{r,\max}\Big) \qquad \text{otherwise} \end{cases}$$

$$\omega_{r,\imath,\mathrm{ref}} = \begin{cases} \dfrac{v_x}{r_{r,\imath}}\Big(1 - \mathcal{F}^{-1}_{x,r,\imath}(F_{x,r,\imath,\mathrm{ref}}(v_x,\omega_{r,\imath}))\Big) \\ \qquad\qquad \text{if } \lambda_{r,\imath} \in [-\lambda_{r,\max},\lambda_{r,\max}] \\ \dfrac{v_x}{r_{r,\imath}}\Big(1 \mp \lambda_{r,\max}\Big) \qquad \text{otherwise} \end{cases} \tag{13}$$

necessary to exert the required longitudinal forces. Therefore, setting $e_{\omega_{r,\ell}} = \omega_{r,\ell} - \omega_{r,\ell,\mathrm{ref}}$, $e_{\omega_{r,\imath}} = \omega_{r,\imath} - \omega_{r,\imath,\mathrm{ref}}$, from (5), one works out

$$\begin{aligned} \dot I_{e_{\omega_{r,\ell}}} &= -\alpha_{2,\ell}\,\mathrm{sign}(e_{\omega_{r,\ell}}) - k_{i,\ell}e_{\omega_{r,\ell}} \\ \dot I_{e_{\omega_{r,\imath}}} &= -\alpha_{2,\imath}\,\mathrm{sign}(e_{\omega_{r,\imath}}) - k_{i,\imath}e_{\omega_{r,\imath}} \\ i_{q,\ell,\mathrm{ref}} &= \frac{1}{p\Phi_\ell}\Big(T_{b,r,\ell} + r_{r,\ell}F_{x,r,\ell} + J_\ell\Big(- \alpha_{1,\ell}\left\lfloor e_{\omega_{r,\ell}}\right\rceil^{1/2} \\ &\quad - k_{p,\ell}e_{\omega_{r,\ell}} + I_{e_{\omega_{r,\ell}}} + \dot\omega_{r,\ell,\mathrm{ref}}\Big)\Big) \\ i_{q,\imath,\mathrm{ref}} &= \frac{1}{p\Phi_\imath}\Big(T_{b,r,\imath} + r_{r,\ell}F_{x,r,\imath} + J_\imath\Big(- \alpha_{1,\imath}\left\lfloor e_{\omega_{r,\imath}}\right\rceil^{1/2} \\ &\quad - k_{p,\imath}e_{\omega_{r,\imath}} + I_{e_{\omega_{r,\imath}}} + \dot\omega_{r,\imath,\mathrm{ref}}\Big)\Big) \end{aligned}$$

with $\alpha_{1,j},\alpha_{2,j},k_{p,j},k_{i,j} > 0$, $4\alpha_{2,j}k_{i,j} > (9\alpha_{1,j}^2 + 8\alpha_{2,j})k_{p,j}^2$, $j = \ell,\imath$, where the PI and super–twisting actions have been applied. Finally, considering the current errors $e_{i_{d,\ell}} = i_{d,\ell} - i_{d,\ell,\mathrm{ref}}$, $e_{i_{q,\ell}} = i_{q,\ell} - i_{q,\ell,\mathrm{ref}}$, $e_{i_{d,\imath}} = i_{d,\imath} - i_{d,\imath,\mathrm{ref}}$, $e_{i_{q,\imath}} = i_{q,\imath} - i_{q,\imath,\mathrm{ref}}$, with $i_{d,\ell,\mathrm{ref}} = 0$, $i_{d,\imath,\mathrm{ref}} = 0$, from (3), one obtains the voltage input to be applied to the PMSMs

$$\begin{aligned} \dot I_{e_{i_{d,\ell}}} &= -\alpha_{2,d,\ell}\,\mathrm{sign}(e_{\omega_{r,\ell}}) - k_{i,d,\ell}e_{\omega_{r,\ell}} \\ \dot I_{e_{i_{q,\ell}}} &= -\alpha_{2,q,\ell}\,\mathrm{sign}(e_{\omega_{r,\ell}}) - k_{i,q,\ell}e_{\omega_{r,\ell}} \\ \dot I_{e_{i_{d,\imath}}} &= -\alpha_{2,d,\imath}\,\mathrm{sign}(e_{\omega_{r,\imath}}) - k_{i,d,\imath}e_{\omega_{r,\imath}} \\ \dot I_{e_{i_{q,\imath}}} &= -\alpha_{2,q,\imath}\,\mathrm{sign}(e_{\omega_{r,\imath}}) - k_{i,q,\imath}e_{\omega_{r,\imath}} \\ v_{d,\ell} &= R_\ell i_{d,\ell} - pL_\ell\omega_{r,\ell}i_{q,\ell} + L_\ell\Big(- \alpha_{1,d,\ell}\left\lfloor e_{i_{d,\ell}}\right\rceil^{1/2} \\ &\quad - k_{p,d,\ell}e_{i_{d,\ell}} + I_{e_{i_{d,\ell}}} + \frac{di_{d,\ell,\mathrm{ref}}}{dt}\Big) \\ v_{q,\ell} &= R_\ell i_{q,\ell} + pL_\ell\omega_{r,\ell}i_{d,\ell} + pL_\ell\Phi_\ell\omega_{r,\ell} \\ &\quad + L_\ell\Big(- \alpha_{1,q,\ell}\left\lfloor e_{i_{q,\ell}}\right\rceil^{1/2} - k_{p,q,\ell}e_{i_{d,\ell}} \\ &\quad + I_{e_{i_{d,\ell}}} + \frac{di_{q,\ell,\mathrm{ref}}}{dt}\Big) \\ v_{d,\imath} &= R_\imath i_{d,\imath} - pL_\ell\omega_{r,\imath}i_{q,\imath} + L_\imath\Big(- \alpha_{1,d,\imath}\left\lfloor e_{i_{d,\imath}}\right\rceil^{1/2} \\ &\quad - k_{p,d,\imath}e_{i_{d,\imath}} + I_{e_{i_{d,\imath}}} + \frac{di_{d,\imath,\mathrm{ref}}}{dt}\Big) \\ v_{q,\imath} &= R_\imath i_{q,\imath} + pL_\imath\omega_{r,\imath}i_{d,\imath} + pL_\imath\Phi_\imath\omega_{r,\imath} \\ &\quad + L_\imath\Big(- \alpha_{1,q,\imath}\left\lfloor e_{i_{q,\imath}}\right\rceil^{1/2} - k_{p,q,\imath}e_{i_{d,\imath}} \\ &\quad + I_{e_{i_{d,\imath}}} + \frac{di_{q,\imath,\mathrm{ref}}}{dt}\Big) \end{aligned}$$

with $\alpha_{1,h,j},\alpha_{2,h,j},k_{p,h,j},k_{i,h,j} > 0$, $4\alpha_{2,h,j}k_{i,h,j} > (9\alpha_{1,h,j}^2 + 8\alpha_{2,h,j})k_{p,h,j}^2$, $j = \ell,\imath$, $h = d,q$.

4. SIMULATION RESULTS

The controller designed in the previous section, has been applied to a vehicle characterized by $m = 1800$ kg, $J_z = 2386$ kg m^2, $l_f = 1.38$ m, $l_r = 1.53$ m, and $t_v = 1.74$ m.

The performance of the controller has been tested making use of a particularly challenging maneuver, the double lane change. It consists of a maneuver in which, at $t = 1$ s, the steering wheel is maintained at $\delta_{d,sw} = +100°$ for 2 seconds, and at $\delta_{d,sw} = -100°$ for other 2 seconds. Finally, it is brought back at $\delta_{d,sw} = 0$ at $t = 5$ s. This signal is filtered by a first order low–pass filter to take into account the steering wheel dynamics (see Fig. 1). The ratio between the steering wheel angle $\delta_{d,sw}$ and δ_d is 16.

The friction coefficient undergoes an abrupt change at $t = 3.5$, passing from $\mu_x = \mu_y = 0.9$ (dry road) to $\mu_x = \mu_y = 0.5$ (wet road), see Fig. 2. A white noise is superimposed to theier values. The tire stiffness coefficients are $D_{y,f} = 8854$, N, $C_{y,f} = 1.41$, $B_{y,f} = 16$, $E_{y,f} = 0$, and $D_{x,r,l} = 8854$, $D_{x,r,r} = 8394$ N, $C_{x,r,l} = 1.41$, $C_{x,r,r} = 1.41$, $B_{x,r,l} = 16$, $B_{x,r,r} = 16$.

Furthermore, the reference generator is characterized by $D_{x,f,\mathrm{ref}} = 10000$, $D_{x,r,\mathrm{ref}} = 10000$ N, $C_{x,f,\mathrm{ref}} = 1.61$, $C_{x,r,\mathrm{ref}} = 1.61$ and $B_{x,f,\mathrm{ref}} = B_{x,r,\mathrm{ref}} = 16$, and $D_{y,f,\mathrm{ref}} = 10000$, $D_{y,r,\mathrm{ref}} = 10000$ N, $C_{y,f,\mathrm{ref}} = 1.61$, $C_{y,r,\mathrm{ref}} = 1.61$ and $B_{y,f,\mathrm{ref}} = B_{y,r,\mathrm{ref}} = 16$. Moreover, $J_{z,\mathrm{ref}} = 2386$ kg m^2 and $m_{\mathrm{ref}} = 1800$ kg.

As far as the PMSMs are concerned, the parameters are $R_\ell = R_\imath = 2.875\ \Omega$, $L_\ell = L_\imath = 0.0085$ H, $\Phi_\ell = \Phi_\imath = 0.175$ Wb, the pole number is $p = 4$, the equivalent radii are

$r_f = 0.28$, $r_{r,\ell} = r_{r,\imath} = 0.25$ m, and the inertia are $J_f = J_r = 0.635$ kg m^2.

The initial longitudinal velocity is $v_x(0) = 28$ m/s. Moreover, $v_y(0) = 0$ m/s and $\omega_z(0) = 0$ rad/s. For the PMSMs, the initial condition to current vectors are $i_{d,\ell}(0) = 0$, $i_{q,\ell}(0) = 0$, $i_{d,\imath}(0) = 0$, $i_{q,\imath}(0) = 0$.

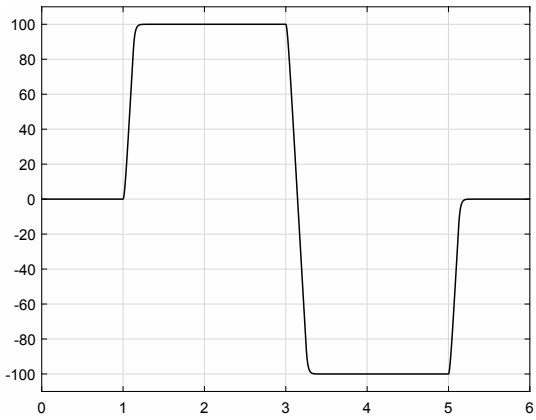

Fig. 1. Steering wheel angle δ_d in the double lane change maneuver [deg vs s].

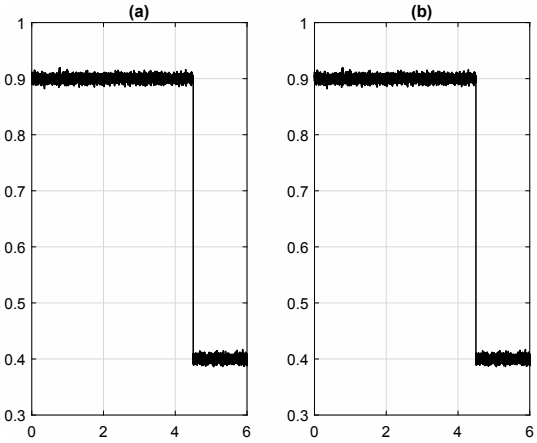

Fig. 2. Vehicle parameters: Friction coefficient a) μ_x; b) μ_y

A disturbance due to the wind, see Figure 3, has been considered to test the robustness against environmental disturbances. The wind has a velocity $v_W = (v_{w,X}, v_{w,Y}, 0)^T$ in the inertial frame RC, with

$$v_{w,X} = V_w \cos(\beta_0 + \Delta\beta_0) + 0.025\, \mathcal{N}$$
$$v_{w,Y} = V_w \sin(\beta_0 + \Delta\beta_0) + 0.025\, \mathcal{N}$$
$$V_w = V_{w,0} + \Delta V_w \sin \omega_w t$$

where $V_{w,0}$ is the nominal wind magnitude, $\beta_0 = -120°$ the nominal angle between the X–axis and the wind vector, $\omega_w = 1.5$ rad/s, $\mathcal{N}$ the uniform distribution, $\Delta\beta_0 = 0.2\, \beta_0$, and $\Delta V_w = 0.1\, V_{w,0}$. In the frame $R\Gamma$ fixed with the vehicle, the wind velocity components are

$$v_{w,x} = v_{w,X} \cos\alpha_z + v_{w,Y} \sin\alpha_z$$
$$v_{w,y} = -v_{w,X} \sin\alpha_z + v_{w,Y} \cos\alpha_z.$$

Combining of the apparent wind velocity, due to the vehicle motion, with the components $v_{w,x}$, $v_{w,y}$, one gets the wing velocity components as $v_{aw,x} = v_x - v_{w,x}$, $v_{aw,y} = v_y - v_{w,y}$. This disturbance determines some longitudinal and lateral forces

$$F_{d,x} = -A_{s,f}\, \varrho c_{a,x} v_{aw,x}^2/2$$
$$F_{d,y} = -A_{s,l}\, \varrho c_{a,y} v_{aw,y}^2/2$$

with $A_{s,f} = 2.59$ m^2, $A_{s,l} = 5.1$ m^2 the front/lateral surfaces of the vehicle, $\varrho = 1.2$ kg/m^3 the air density, and $c_{a,x} = 0.3$, $c_{a,y} = 0.6$ the (dimensionless) front/lateral aerodynamic coefficients. Moreover, the wind determines a pitching moment about the y direction (neglected), a roll moment in the x direction (neglected), and a yaw moment $M_{d,z} = l_c F_{d,y}$, assumed given by $F_{d,y}$ multiplied by the distance $l_c = l_{c0} + 0.025\, \mathcal{N}$ of the vehicle center of mass and the wind center of pressure, where $l_{c0} = -0.20$ m is its nominal value.

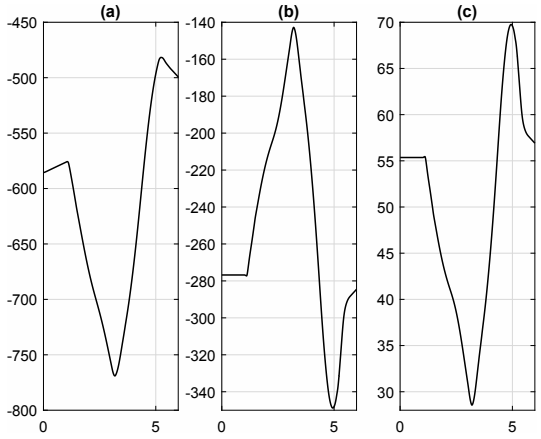

Fig. 3. Vehicle parameters: a) Disturbance $F_{d,x}$ [N vs s]; b) Disturbance $F_{d,y}$ [N vs s]; c) Disturbance $M_{d,z}$ [N m vs s].

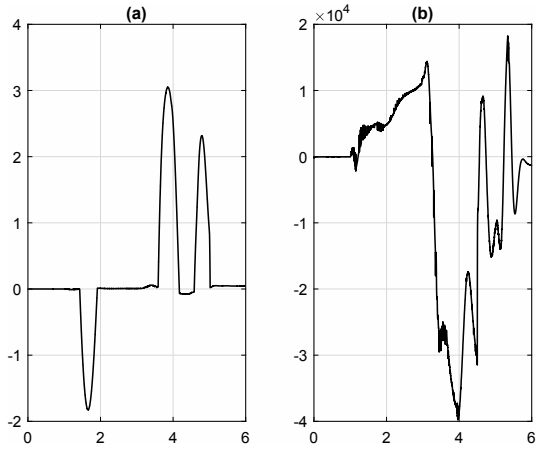

Fig. 4. Vehicle parameters: a) AFS input δ_c [deg vs s]; b) RTV input M_z [N m vs s]

The control gains for the active control are $k_{p,x} = 50$, $k_{i,x} = 30$, $k_{p,y} = 200$, $k_{i,y} = 145$, $k_{p,z} = 150$, $k_{i,z} = 100$, $\alpha_{1,x} = 0.1$, $\alpha_{2,x} = 0.05$, $\alpha_{1,y} = 0.1$, $\alpha_{2,y} = 0.05$, $\alpha_{1,z} = 0.1$, $\alpha_{2,z} = 0.05$. Finally, the control gains for the PMSM control are $k_{p,d,\ell} = 10$, $k_{i,d,\ell} = 1.2 k_{p,d,\ell}$, $k_{p,q,\ell} = 50$, $k_{i,q,\ell} = 10 k_{p,q,\ell}$, $k_{p,d,\imath} = 100$, $k_{i,d,\imath} = 10 k_{p,d,\imath}$, $k_{p,q,\imath} = 100$, $k_{i,q,\imath} = 10 k_{p,q,\imath}$, $\alpha_{1,\ell} = \alpha_{1,\imath} = 0.01$, $\alpha_{2,\ell} = \alpha_{2,\imath} = 0.005$, $\alpha_{1,d,\ell} = \alpha_{1,d,\imath} = \alpha_{1,q,\ell} = \alpha_{1,q,\imath} = 0.001$, $\alpha_{2,d,\ell} = \alpha_{2,d,\imath} = \alpha_{2,q,\ell} = \alpha_{2,q,\imath} = 0.0005$.

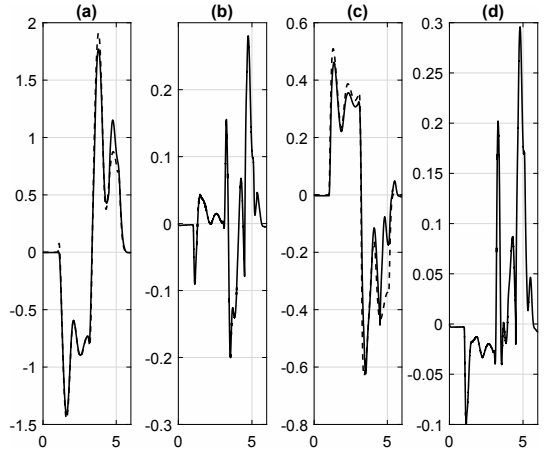

Fig. 5. a) Lateral velocity v_y (black) and reference $v_{y,\text{ref}}$ (dash) [m/s vs s]; b) Tracking error $e_{v_y} = v_y - v_{y,\text{ref}}$ [m/s vs s]; c) Lateral velocity ω_z (black) and reference $\omega_{z,\text{ref}}$ (dash) [rad/s vs s]; d) Tracking error $e_{\omega_z} = \omega_z - \omega_{z,\text{ref}}$ [rad/s vs s]

Figs. 5 show v_y, ω_z along with the references $v_{y,\text{ref}}, \omega_{z,\text{ref}}$ to be tracked, and the tracking errors $v_y - v_{y,\text{ref}}$, $\omega_z - \omega_{z,\text{ref}}$. It is possible to observe that the proposed controller ensures small tracking errors (see Figs. 5.b, d). The active controls δ_c, due to the AFS, and M_z, due to the PMSMs, are shown in Fig. 4. Figs. 6. show the current behaviour. The proposed controller ensures the tracking of the references $i_{d,\ell,\text{ref}}$, $i_{q,\ell,\text{ref}}$, $i_{d,\imath,\text{ref}}$, $i_{q,\imath,\text{ref}}$. The voltage controls $v_{d,\ell}$, $v_{q,\ell}$, $v_{d,\imath}$, $v_{q,\imath}$, are shown in Fig. 7.

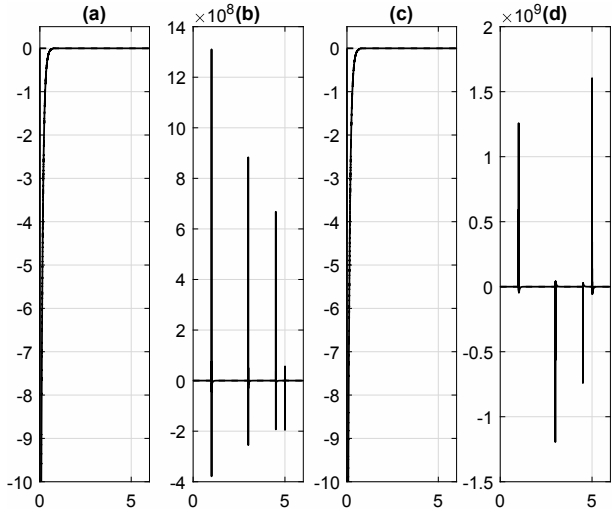

Fig. 6. a) Current vector $i_{d,\ell}$ (black) and reference $i_{d,\ell,\text{ref}}$ (dash) [Amp vs s]; b) Current vector $i_{q,\ell}$ (black) and reference $i_{q,\ell,\text{ref}}$ (dash) [Amp vs s]; c) Current vector $i_{d,\imath}$ (black) and reference $i_{d,\imath,\text{ref}}$ (dash) [Amp vs s]; d) Current vector $i_{q,\imath}$ (black) and reference $i_{q,\imath,\text{ref}}$ (dash) [Amp vs s]

5. CONCLUSIONS

In this work, an integrated active chassis controller has been designed for an electric vehicle equipped with PMSMs, mounted on the rear axel. These motors provide not only the longitudinal traction, but also the active yaw torque which, along with the AFS, can realize the active chassis control of the vehicle.

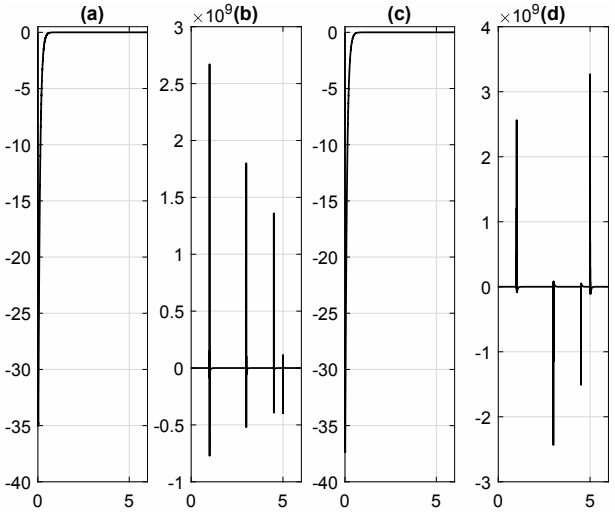

Fig. 7. Voltage vectors a) $v_{d,\ell}$ [V vs s]; b) $v_{q,\ell}$ [V vs s]; c) $v_{d,\imath}$ [V vs s]; d) $v_{q,\imath}$ [V vs s]

This paper represents a first advance on this subject, and work is in progress to render this controller robust with respect to parameter uncertainties and external perturbations, as well as to obtain its digital version implementable on digital devices.

REFERENCES

Y. Hori, Future Vehicle Driven by Electricity and Control – Research on Four–Wheel–Motored 'UOT March II', *IEEE Transactions on Industrial Electronics*, Vol. 51, No. 5, pp. 954–962, 2004.

R. Wang, Y. Chen, D. Feng, X. Huang, and J. Wang, Development and Performance Characterization of an Electric Ground Vehicle with Independently Actuated in–Wheel Motors, *Journal of Power Sources*, Vol. 196, No. 8, pp. 3962–3971, 2011.

Z. Shuai, H. Zhang, J. Wang, J. Li, and M. Ouyang, Combined AFS and DYC Control of Four–Wheel–Independent–Drive Electric Vehicles over CAN Network with Time–Varying Delays, *IEEE Transactions on Vehicular Technology*, Vol. 63, No. 2, pp. 591–602, 2014.

J. Ni, J. Hu, and C. Xiang, Envelope Control for Four–Wheel Independently Actuated Autonomous Ground Vehicle through AFS/DYC Integrated Control, *IEEE Transactions on Vehicular Technology*, Vol. 66, No. 11, pp. 9712–9726, 2017.

X. Ji, X. He, C. Lv, Y. Liu, and Jian Wu. A Vehicle Stability Control Strategy with Adaptive Neural Network Sliding Mode Theory Based on System Uncertainty Approximation, *Vehicle System Dynamics*, Vol. 56, No. 6, pp. 923–946, 2018.

C. Acosta–Lúa, B. Castillo–Toledo, and S. Di Gennaro, and A. Toro, Nonlinear Robust Regulation of Ground Vehicle Motion, *Proceedings of the* 46^{th} *IEEE Conference on Decision and Control*, New Orleans, pp. 3871–3876, 2007.

C. Acosta–Lúa, B. Castillo–Toledo, and S. Di Gennaro, Nonlinear Output Robust Regulation of Ground Vehicles in Presence of Disturbances and Parameter Uncertainties, *Proceedings of the* 17^{th} *IFAC World Congress*, Seoul, Korea, July 6–11, pp. 141–146, 2008.

C. Acosta Lúa, B. Castillo-Toledo, R. Cespi, S. Di Gennaro, An Integrated Active Nonlinear Controller for Wheeled Vehicles, *Journal of the Franklin Institute*, vol. 352, no. 11, pp. 4890–4910, 2015.

C. Acosta Lúa, and S. Di Gennaro, Nonlinear Adaptive Tracking for Ground Vehicles in the Presence of Lateral Wind Disturbances and Parameter Variations, *Journal of the Franklin Institute*, Vol. 354, pp. 2742–2768, 2017.

C. Acosta Lúa S. Di Gennaro, A. Navarrete Guzman, S. Ortega Cisneros, and J. Rivera Domínguez, Digital Implementation via FPGA of Controllers for Active Control of Ground

Vehicles, *IEEE Transactions on Industrial Informatics*, Early Access. Print ISSN: 1551-3203. Online ISSN: 1941-0050. DOI: 10.1109/TII.2019.2890839.

D. Bianchi, A. Borri, G. Burgio, M. D. Di Benedetto, and S. Di Gennaro, Adaptive Integrated Vehicle Control using Active Front Steering and Rear Torque Vectoring, *Proceedings of the* 48^{th} *IEEE Conference on Decision and Control*, Shanghai, Cina, pp. 3557–3562, 2009.

D. Bianchi, A. Borri, G. Burgio, M. D. Di Benedetto, and S. Di Gennaro, Adaptive Integrated Vehicle Control using Active Front Steering and Rear Torque Vectoring, *International Journal of Vehicle Autonomous Systems*, Special Issue on: "Autonomous and Semi–Autonomous Control for Safe Driving of Ground Vehicles", Vol. 8, No. 2/3/4, pp. 85–105, 2010.

D. Bianchi, A. Borri, B. Castillo–Toledo, M.D. Di Benedetto, and S. Di Gennaro, Active Control of Vehicle Attitude with Roll Dynamics, *Proceedings of the* 18^{th} *IFAC World Congress*, Milan, Italy, pp. 7174–7179, 2011.

G. Burgio, B. Castillo–Toledo and S. Di Gennaro, Nonlinear Adaptive Tracking for Ground Vehicles, *Proceedings of the* 48^{th} *IEEE Conference on Decision and Control*, Shanghai, Cina, pp. 7645–7650, 2009.

A. Borri, D. Bianchi, M. D. Di Benedetto, and S. Di Gennaro, Optimal Workload Actuator Balancing and Dynamic Reference Generation in Active Vehicle Control, *Journal of the Franklin Institute*, Vol. 354, pp. 1722–1740, 2017.

L. Etienne, S. Di Gennaro, J.P. Barbot, Active Ground Vehicle Control with Use of a Super–Twisting Algorithm in the Presence of Parameter Variations, *Proceedings of the* 3^{rd} *International Conference on Systems and Control (ICSC)*, pp. 1134–1139, 2013.

M. Martinez–Gardea, I.J. Mares Guzmán, Cuauhtémoc Acosta Lúa, S. Di Gennaro, and Ivan Vázquez Álvarez, Design of a NonLinear Observer for a Laboratory Antilock Braking System, *Control Engineering and Applied Informatics*, Vol. 17, No. 3, pp. 105–112, 2015.

L. Etienne, C. Acosta Lúa, S. Di Gennaro, and J.P. Barbot, A Super–Twisting Controller for Active Control of Ground Vehicles with Tire–Road Friction Estimation and CarSim Validation, *International Journal of Control, Automation and Systems*, Submitted, 2019.

D. Kim, S. Hwang, and H. Kim, Vehicle Stability Enhancement of Four–Wheel–Drive Hybrid Electric Vehicle Using Rear Motor Control, *IEEE Transactions on Vehicular Technology*, Vol. 57, No. 2, pp. 727–735, 2008.

H. Kim, J. Park, K. Jeon, and S. Choi, Integrated Control Strategy for Torque Vectoring and Electronic Stability Control for in Wheel Motor EV, *2013 World Electric Vehicle Symposium and Exhibition (EVS27)*, pp. 1–7, 2013.

C. Fu, R. Hoseinnezhad, K. Li, M. Hu, F. Huang, and F. Li, Vehicle Integrated Chassis Control via Multi–Input Multi–Output Sliding Mode Control, *2018 International Conference on Control, Automation and Information Sciences (ICCAIS)*, pp. 355–360, 2018.

X. Liu–Henke, M. Göllner, M. Fritsch, R. Feind, and R. Buchta, FreDy – An Electric Vehicle with Intelligent Chassis–Control Systems, *2015 Tenth International Conference on Ecological Vehicles and Renewable Energies (EVER)*, pp. 1–8, 2015.

T. Ming, W. Deng, and Y. Wang, Integrated Chassis Control with Optimal Tire Force Distribution for Electric Vehicles, *2015 IEEE International Conference on Systems, Man, and Cybernetics*, pp. 2504–2509, 2015.

L. Zhang, H. Ding, K. Guo, J. Zhang, W. Pan, and Z. Jiang, Cooperative chassis control system of electric vehicles for agility and stability improvements, *IET Intelligent Transport Systems*, Vol. 13, No. 1, pp. 134–140, 2019.

C. Lv, X. Hu, A. Sangiovanni–Vincentelli, Y. Li, C. Marina-Martinez, and D. Cao, Driving–Style–Based Co–Design Optimization of an Automated Electric Vehicle: A CyberPhysical System Approach, *IEEE Transactions on Industrial Electronics*, Vol. 66, No. 4, pp. 2965–2975, 2019.

P. Krause, O. Wasynczuk, T. O'Connell, and M. Hasan, Introduction to Electric Power and Drive Systems, Wiley, 2017.

W. Leonard, *Control of Electrical Drives*, Berlin, Springer–Verlag, 1985.

R.H. Park, Two–Reaction Theory of Synchronous Machines – Generalized Method of Analysis – Part I, *AIEE Transactions*, Vol. 48, pp. 716–727, 1929.

H.B. Pacejka, *Tyre and Vehicle Dynamics*, Elsevier Butterworth–Hein, 2005.

J. Wong. Theory of Ground Vehicles; New York, Wiley, 1978.

C. Edwards, and S.K. Spurgeon, *Sliding Mode Control: Theory and Application 1999*, Taylor and Francis Ltd., London.

G. Bartolini, A. Pisano, and E. Usai, First and Second Derivative Estimation by Sliding Mode Technique, *Journal of Signal Processing*, No. 4, pp. 167–176, 2000.

L. Fridman, and A. Levant, Higher Order Sliding Modes, in *Sliding Mode Control in Engineering*, Marcel Dekker, New York, pp. 53–101, 2002.

T. Floquet, and J–P. Barbot, Super Twisting Algorithm based Step–by–Step Sliding Mode Observers for Nonlinear Systems with Unknown Inputs, in: *Special Issue of International Journal of Systems Science on Advances in Sliding Mode Observation and Estimation*, Vol. 10, No. 10, pp. 803–815, 2007.

A. Levant, Higher–Order Sliding Modes, Differentiation and Output Feedback Control, *International Journal of Control*, Vol. 76, No. 9, 10, pp. 924–941, 2003.

L. Fridman, Y. Shtessel, C. Edwards, X.G. Yan, Higher–Order Sliding–Mode Observer for State Estimation and Input Reconstruction in Nonlinear Systems, *International Journal of Robust and Nonlinear Control*, Vol. 18, No. 4, 5, pp. 399–413, 2008.

A. Levant, Homogeneity Approach to High–Order Sliding Mode Design, *Automatica*, Vol. 41, No. 5, pp. 823–830, 2005.

J. A. Moreno and M. Osorio, A Lyapunov Approach to Second–Order Sliding Mode Controllers and Observers, *Proceedings of the* 47^{th} *IEEE Conference on Decision and Control*, Cancun, Mexico, pp. 2856–2861, 2008.

M.V. Basin, P. Yu, Y.B. Shtessel, Hypersonic Missile Adaptive Sliding Mode Control Using Finite– and Fixed–Time Observers, *IEEE Transactions on Industrial Electronics*, Vol. 65, No. 1, pp. 930–941, 2018.

H. Deng, Q. Li, W. Chen, G. Zhang, High–Order Sliding Mode Observer Based OER Control for PEM Fuel Cell Air–Feed System, *IEEE Transactions on Energy Conversion*, Vol. 33, No. 1, pp. 232–44, 2018.

Kommuri SK; Lee SB, Veluvolu KC. Robust Sensors–Fault–Tolerance With Sliding Mode Estimation and Control for PMSM Drives. IEEE/ASME Transactions on Mechatronics, Vol. 23, No. 1, pp. 17–28, 2018.

Pan Y, Yang C, Pan L, Yu H. Integral Sliding Mode Control: Performance, Modification, and Improvement. IEEE Transactions on Industrial Informatics, Vol. 14, No. 7, pp. 3087–96, 2018.

Panathula CB, Rosales A, Shtessel YB, Fridman LM. Closing Gaps for Aircraft Attitude Higher Order Sliding Mode Control Certification via Practical Stability Margins Identification. IEEE Transactions on Control Systems Technology, Vol. 26, No. 6, pp. 2020–34, 2018.

Liu J, Gao Y, Su X, Wack M, Wu L. Disturbance Observer Based Control for Air Management of PEM Fuel Cell Systems via Sliding Mode Technique. IEEE Transactions on Control Systems Technology, pp. 1–10, 2018.

Gao Y., Liu J, Sun G, Liu M, Wu L. Fault Deviation Estimation and Integral Sliding Mode Control Design for Lipschitz Nonlinear Systems. Systems & Control Letters, Vol. 123, pp. 8–15, 2019.

Van M. An Enhanced Tracking Control of Marine Surface Vessels Based on Adaptive Integral Sliding Mode Control and Disturbance Observer. ISA Transactions, In Press, 2019.